PERGAMON

Mechanism and Machine Theory 35 (2000) 1269–1285

MECHANISM AND MACHINE THEORY

www.elsevier.com/locate/mechmt

Drive train design of redundant-drive backlash-free robotic mechanisms

Dar-Zen Chen*, Kang-Li Yao

Department of Mechanical Engineering, National Taiwan University, Taipei, Taiwan

Received 1 August 1998; accepted 10 July 1999

Abstract

This paper describes a systematic methodology for the drive train design of redundant-drive backlash-free robotic mechanisms (RBR mechanisms). A two-stage procedure that involves the selection of drive train configurations and the determination of gear ratios is presented. It is shown that proper gear train configurations associated with the inner structure matrix can be determined by the given inertia characteristics of primary links, while those associated with the outer structure matrix can be determined from the unidirectional drive characteristics of the RBR mechanism. Conditions determining gear ratios such that the RBR mechanism can have optimum dynamic performance are also derived. From the selected gearing configuration's and determined gear ratios, the locations of motors and arrangements of drive trains can be laid out accordingly. A 3-dof RBR mechanism is used as an illustrative example.

Keywords: Drive train design; Redundant-drive backlash-free manipulator; Gear ration determination

1. Introduction

It is known that conventional gears have a certain amount of backlash to ensure proper gear meshing, and to prevent jamming of gear teeth due to manufacturing error or thermal expansion. However, backlash introduces discontinuity, uncertainty, and impact in mechanical systems which makes accurate control of a manipulator difficult. Chang and Tsai [3]

* Corresponding author. Tel.: +886-2-362-1522; fax: +886-2-763-1755.
E-mail address: dzchen@ccms.ntu.edu.tw (D.-Z. Chen).

0094-114X/00/$ - see front matter
PII: S0094-114X(99)00066-X

introduced the redundant unidirectional drive concept to eliminate the backlash effect. They showed that by applying at least two opposite unidirectional torques on each joint, the effect of backlash due to torque reversal can be eliminated. Furthermore, with the redundant motors, a redundant-drive backlash-free robotic (RBR) mechanism has the fail–safe advantage when one of its unidirectional drive fails.

Chen and Tsai [6] developed a methodology to determine the gear ratios of a 2 degree-of-freedom (dof) geared robotic mechanism such that the mechanism can possess kinematic isotropic property and optimum dynamic performance. Chen and Tsai [7] showed that through proper choice of gear ratios, manipulators can be made with maximum acceleration capacity when the reflected inertia of input links represented at the joint-space is equal to that of primary links. Chen [4] addressed the compatibility problem between the structure and Jacobian matrices of an articulated gear mechanism and derived the conditions for the drive train design based on the generalized principle of inertia match. Chen [5] extended the optimum dynamic performance condition from 2-dof manipulators to 3-dof manipulators. However, these studies are limited only to the case where the number of dof of a manipulator is equal to the number of motors, and the applicability on the redundant-drive mechanisms was not addressed.

In this paper, a methodology for the drive train design of RBR mechanisms will be presented. The design problem is treated as the selection of drive train configurations and the determination of gear ratios such that the mechanism can have optimum dynamic performance. It is shown that proper gear train configurations associated with the inner structure matrix can be determined by the given inertia characteristics of primary links, while those associated with the outer structure matrix can be determined from the unidirectional drive characteristics of the RBR mechanism. Conditions to determine gear ratios based on the maximum acceleration capacity are presented. From the selected gearing configurations and determined gear ratios, the locations of motors and arrangements of drive trains can be laid out accordingly. A 3-dof RBR mechanism is used as an illustrative example.

2. RBR mechanism

In graphical representation, links are denoted by vertices and joints by edges, turning pairs by thin edges, and gear pairs by heavy edges. By rearranging coaxial revolute joints, a unique canonical graph representation [11] can be obtained. In the canonical graph representation, all edges lying on a thin-edge path traced from the base to any other vertex have different edge labels. Among these thin-edge paths, the linkage that starts from the base link and ends at the output links is defined as the equivalent open-loop chain (EOLC) [11]. Each link in the EOLC is referred to as a primary link, while all other links are called secondary links [7]. The arrangement of secondary links, which describes where the motors are located and how the input torques are transmitted to various joints of the mechanism, forms the mechanical transmission lines [2]. The torque vectors at actuator-space and joint-space are related by the structure matrix $\mathbf{A}$ [2] as

$$\tau = \mathbf{A}\xi \tag{1}$$

where the elements of **A** are functions of gear ratios, τ and ξ are torque vectors at the joint-space and actuator-space, respectively.

From Eq. (1), it can be seen that the jth row of **A** describes how the resultant torque at joint "j" is affected by the input links, while the kth column of **A** describes how the torque of motor k is transmitted to various joints of a mechanism. Hence, the gear train which results in a series of non-zero elements in the kth column of **A** forms the mechanical transmission line for motor k. And the (j, k) element of **A** represents how the torque of motor k is transmitted to joint "j" of the mechanism.

Chang and Tsai [3] showed that the structure matrix **A** of an RBR mechanism has the following characteristics:

C1. Each row of **A** contains at least two non-zero elements which ensures that there are at least two torques applied on each joint.
C2. Sub-matrices obtained by removing any column of **A** are non-singular.
C3. Non-zero elements in any column of **A** are consecutive.
C4. Switching any two columns of **A** results in an isomorphic structure.

With these characteristics, Chang and Tsai [3] enumerated four admissible structure matrices for 2-dof RBR mechanisms with three inputs, and 34 admissible structure matrices for 3-dof RBR mechanisms with four inputs. Tables 1 and 2 show the admissible structure matrices for 2- and 3-dof RBR mechanisms, respectively. These matrices are labeled according to the location of the motors. The letters "g", "s", and "e", respectively, denote the locations of the motors at the 1st, 2nd, and 3rd joint axes, which are corresponding to the ground, shoulder, and elbow joints of a robot arm. Among these available structure matrices, the g^4-series have all four motors mounted on the ground, the g^3s-series have three motors mounted on the ground and one on primary link 1, and so forth.

Fig. 1 shows the functional representation of a 3-dof mechanism with four inputs. Links 4, 5, 8, and 9 are input links and link 3 is the output link. Motors 1, 2, 3, and 4 are attached to input links 4, 5, 8, and 9, respectively, to drive the mechanism. In Fig. 1, orientations of axes a, d, g, and h are assumed positive upward, while orientations of axes b, c, e, and f are assumed positive to the right. Fig. 2 shows the associated canonical graph representation. From Fig. 2, it can be seen that links 0, 1, 2, and 3 are primary links; and links 4, 5, 6, 7, 8, 9, 10, and 11 are secondary links. The torque vectors at actuator-space and joint-space can be derived by using fundamental circuit theory and coaxial conditions [11] as

Table 1
Admissible structure matrices for 2-dof RBR mechanisms

$\begin{bmatrix}\# & \# & \#\\ \# & \# & \#\end{bmatrix}$	$\begin{bmatrix}\# & \# & \#\\ \# & \# & 0\end{bmatrix}$	$\begin{bmatrix}\# & \# & 0\\ \# & \# & \#\end{bmatrix}$	$\begin{bmatrix}\# & \# & 0\\ \# & 0 & \#\end{bmatrix}$
g^3-1	g^3-2	g^2s-1	g^2s-2

$$\begin{bmatrix} \tau_{10} \\ \tau_{21} \\ \tau_{32} \end{bmatrix} = \mathbf{A} \cdot \begin{bmatrix} \xi_4 \\ \xi_5 \\ \xi_8 \\ \xi_9 \end{bmatrix} \tag{2}$$

where

Table 2
Admissible structure matrices for 3-dof RBR mechanisms

$\begin{bmatrix}\#&\#&\#&\#\\\#&\#&\#&\#\\\#&\#&\#&\#\end{bmatrix}$ g^4-1	$\begin{bmatrix}\#&\#&\#&\#\\\#&\#&\#&\#\\\#&\#&\#&0\end{bmatrix}$ g^4-2	$\begin{bmatrix}\#&\#&\#&\#\\\#&\#&\#&0\\\#&\#&\#&0\end{bmatrix}$ g^4-3	$\begin{bmatrix}\#&\#&\#&\#\\\#&\#&\#&\#\\\#&\#&0&0\end{bmatrix}$ g^4-4	$\begin{bmatrix}\#&\#&\#&\#\\\#&\#&\#&0\\\#&\#&0&0\end{bmatrix}$ g^4-5
$\begin{bmatrix}\#&\#&\#&0\\\#&\#&\#&\#\\\#&\#&\#&\#\end{bmatrix}$ g^3s-1	$\begin{bmatrix}\#&\#&\#&0\\\#&\#&\#&\#\\\#&\#&\#&0\end{bmatrix}$ g^3s-2	$\begin{bmatrix}\#&\#&\#&0\\\#&\#&\#&\#\\\#&\#&0&\#\end{bmatrix}$ g^3s-3	$\begin{bmatrix}\#&\#&\#&0\\\#&\#&\#&\#\\\#&\#&0&0\end{bmatrix}$ g^3s-4	$\begin{bmatrix}\#&\#&\#&0\\\#&\#&\#&\#\\\#&0&0&\#\end{bmatrix}$ g^3s-5
$\begin{bmatrix}\#&\#&\#&0\\\#&\#&0&\#\\\#&\#&0&\#\end{bmatrix}$ g^3s-6	$\begin{bmatrix}\#&\#&\#&0\\\#&\#&0&\#\\\#&\#&0&0\end{bmatrix}$ g^3s-7	$\begin{bmatrix}\#&\#&\#&0\\\#&\#&0&\#\\\#&0&0&\#\end{bmatrix}$ g^3s-8		
$\begin{bmatrix}\#&\#&\#&0\\\#&\#&\#&0\\\#&\#&\#&\#\end{bmatrix}$ g^3e-1	$\begin{bmatrix}\#&\#&\#&0\\\#&\#&\#&0\\\#&\#&0&\#\end{bmatrix}$ g^3e-2	$\begin{bmatrix}\#&\#&\#&0\\\#&\#&0&0\\\#&\#&0&\#\end{bmatrix}$ g^3e-3	$\begin{bmatrix}\#&\#&\#&0\\\#&\#&\#&0\\\#&0&0&\#\end{bmatrix}$ g^3e-4	$\begin{bmatrix}\#&\#&\#&0\\\#&\#&0&0\\\#&0&0&\#\end{bmatrix}$ g^3e-5
$\begin{bmatrix}\#&\#&0&0\\\#&\#&\#&\#\\\#&\#&\#&\#\end{bmatrix}$ g^2s^2-1	$\begin{bmatrix}\#&\#&0&0\\\#&\#&\#&\#\\\#&\#&\#&0\end{bmatrix}$ g^2s^2-2	$\begin{bmatrix}\#&\#&0&0\\\#&\#&\#&\#\\\#&0&\#&\#\end{bmatrix}$ g^2s^2-3	$\begin{bmatrix}\#&\#&0&0\\\#&\#&\#&\#\\\#&0&\#&0\end{bmatrix}$ g^2s^2-4	$\begin{bmatrix}\#&\#&0&0\\\#&\#&\#&\#\\0&0&\#&\#\end{bmatrix}$ g^2s^2-5
$\begin{bmatrix}\#&\#&0&0\\\#&0&\#&\#\\\#&0&\#&\#\end{bmatrix}$ g^2s^2-6	$\begin{bmatrix}\#&\#&0&0\\\#&0&\#&\#\\\#&0&\#&0\end{bmatrix}$ g^2s^2-7	$\begin{bmatrix}\#&\#&0&0\\\#&0&\#&\#\\0&0&\#&\#\end{bmatrix}$ g^2s^2-8		
$\begin{bmatrix}\#&\#&0&0\\\#&\#&\#&0\\\#&\#&\#&\#\end{bmatrix}$ g^2se-1	$\begin{bmatrix}\#&\#&0&0\\\#&\#&\#&0\\\#&\#&0&\#\end{bmatrix}$ g^2se-2	$\begin{bmatrix}\#&\#&0&0\\\#&\#&\#&0\\\#&0&\#&\#\end{bmatrix}$ g^2se-3	$\begin{bmatrix}\#&\#&0&0\\\#&0&\#&0\\\#&0&\#&\#\end{bmatrix}$ g^2se-4	$\begin{bmatrix}\#&\#&0&0\\\#&\#&\#&0\\\#&0&0&\#\end{bmatrix}$ g^2se-5
$\begin{bmatrix}\#&\#&0&0\\\#&\#&\#&0\\0&0&\#&\#\end{bmatrix}$ g^2se-6	$\begin{bmatrix}\#&\#&0&0\\\#&0&\#&0\\0&0&\#&\#\end{bmatrix}$ g^2se-7	$\begin{bmatrix}\#&\#&0&0\\\#&0&\#&0\\\#&0&0&\#\end{bmatrix}$ g^2se-8		

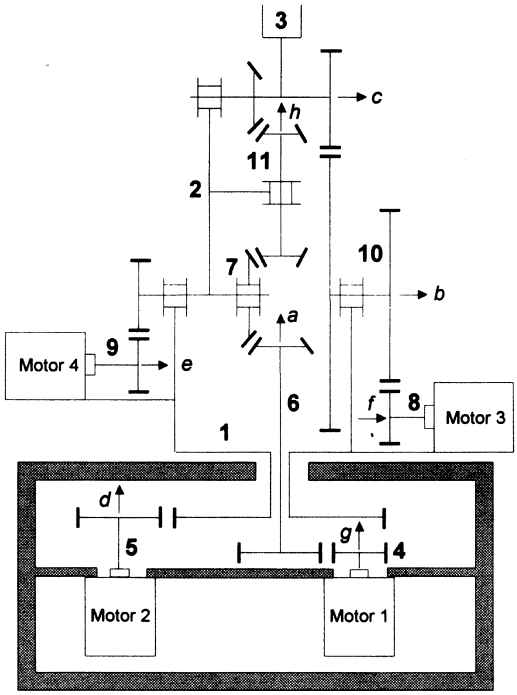

Fig. 1. A 3-dof mechanism with four inputs.

$$\mathbf{A} = \begin{bmatrix} \gamma_{6,4} & \gamma_{1,5} & 0 & 0 \\ \gamma_{6,4} \cdot \gamma_{7,6'} & 0 & \gamma_{10,8} & \gamma_{2,9} \\ \gamma_{6,4} \cdot \gamma_{7,6'} \cdot \gamma_{11,7'} \cdot \gamma_{3,11'} & 0 & \gamma_{10,8} \cdot \gamma_{3,10'} & 0 \end{bmatrix} \tag{3}$$

and $\gamma_{i,j} = \pm N_i/N_j$ denotes the gear ratio for the gear mounted on links i and j, the positive or negative sign varies accordingly as a positive rotation of gear i results in a positive or negative rotation of gear j about their pre-defined axes of rotation, and N_i is the number of teeth on gear i.

From Eq. (3), structure matrix **A** can be considered as a product of two-stage gear reductions and can be rewritten as

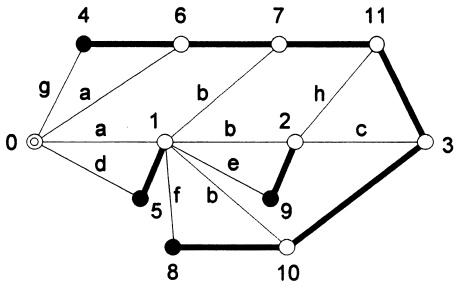

Fig. 2. Canonical graph representation.

$$\mathbf{A} = \mathbf{A}_{\mathrm{i}}\mathbf{A}_{\mathrm{o}} \tag{4}$$

where $\mathbf{A}_{\mathrm{o}}$, a diagonal matrix with its diagonal elements denoted as $a_{k,\,k}$, is called the outer structure matrix and can be written as

$$\mathbf{A}_{\mathrm{o}} = \begin{bmatrix} \gamma_{6,\,4} & 0 & 0 & 0 \\ 0 & \gamma_{1,\,5} & 0 & 0 \\ 0 & 0 & \gamma_{10,\,8} & 0 \\ 0 & 0 & 0 & \gamma_{2,\,9} \end{bmatrix} = \begin{bmatrix} a_{1,\,1} & 0 & 0 & 0 \\ 0 & a_{2,\,2} & 0 & 0 \\ 0 & 0 & a_{3,\,3} & 0 \\ 0 & 0 & 0 & a_{4,\,4} \end{bmatrix} \tag{5a}$$

and $\mathbf{A}_{\mathrm{i}}$ is the inner structure matrix which can be written as

$$\mathbf{A}_{\mathrm{i}} = \begin{bmatrix} 1 & 1 & 0 & 0 \\ \gamma_{7,\,6'} & 0 & 1 & 1 \\ \gamma_{7,\,6'} \cdot \gamma_{11,\,7'} \cdot \gamma_{3,\,11'} & 0 & \gamma_{3',\,10'} & 0 \end{bmatrix} = \begin{bmatrix} 1 & 1 & 0 & 0 \\ b_{2,\,1} & 0 & 1 & 1 \\ b_{3,\,1} & 0 & b_{3,\,3} & 0 \end{bmatrix} \tag{5b}$$

Note that the (k, k) element of the outer structure matrix $\mathbf{A}_{\mathrm{o}}$, $a_{k,\,k}$, is the first non-zero element of the mechanical transmission line for motor k. Also note that from Eqs. (3) and (5b), the form of inner structure matrix is the same as that of the structure matrix. The first non-zero element of each column of the inner structure matrix $\mathbf{A}_{\mathrm{i}}$, which is equal to one, indicates the first joint affected by the associated motor. The other non-zero element of the inner structure matrix $\mathbf{A}_{\mathrm{i}}$, $b_{j,\,k}$, denotes the ratio between the torque contributed by motor k at joint "j" and that at the first joint. Hence, the sign of $b_{j,\,k}$ provides the directional relation between torques at joint "j" and that at the first joint associated with motor k.

3. Generalized principle of inertia match

The acceleration capacity is defined to indicate the ability of a manipulator to respond to a given set of input torques [7]. The larger the acceleration capacity, the more responsive the system is. The generalized principle of inertia match [7] showed that the acceleration capacity can be maximized if the following condition holds

$$I_{\mathrm{m}}\mathbf{A}\mathbf{U}\mathbf{A}^{\mathrm{T}} = \mathbf{M}_{\mathrm{p}} \tag{6}$$

where

$$I_{\mathrm{m}} = \left(\prod_{i=1}^{n} I_i\right)^{1/n} \tag{7}$$

while I_{i} is the mass moment of inertia of the ith input link, $\mathbf{U}$ is a diagonal scaling matrix with (i, i) element equal to $I_{\mathrm{i}}/I_{\mathrm{m}}$ and its determinant equal to unity, $\mathbf{M}_{\mathrm{p}}$ is the inertia matrix of the primary links.

Hence, for an n-dof RBR mechanism to achieve the maximum acceleration capacity, the inertia matrix of the input links reflected at the joint-space is matched with that of the primary links.

4. Compatibility condition

Eq. (6) can be used for the drive train design of RBR mechanisms. Assuming that the kinematic structure of the EOLC has been selected from the geometric consideration, the mass inertia properties of primary links of the RBR mechanism can be estimated and the mass inertia matrix $\mathbf{M}_p$ can be determined at a given posture [8]. The problem now is how to select proper gear train configurations and proper gear ratios such that the maximum acceleration capacity can be achieved.

For an n-dof RBR mechanism, Eq. (6) yields $n(n+1)/2$ non-linear equations. However, the number of unknowns in Eq. (6) depends on the arrangement of the mechanical transmission lines, i.e., the number of non-zero elements in the structure matrix. Obviously, the number of unknowns must be greater than the number of equations available to ensure the solvability of Eq. (6). If the number of unknowns is greater than the number of equations, there must exist some free choices among the non-zero elements in the chosen structure matrix. This leads to the following axiom.

Axiom 1. For an n-dof RBR mechanism to possess maximum acceleration capacity property at a given posture, only those structure matrices with the following characteristics can be chosen as possible gear train configurations if none of the elements in the mass inertia matrix $\mathbf{M}_p$ is equal to zero: (1) none of the elements in the matrix $\mathbf{A}\mathbf{A}^T$ is zero, and (2) the number of non-zero elements in structure matrix $\mathbf{A}$ is greater than $n(n+1)/2$.

For the case that certain element of the mass inertia matrix $\mathbf{M}_p$ is equal to zero at a given posture, the corresponding element in $\mathbf{A}\mathbf{A}^T$ must vanish for Eq. (6) to be solvable. Note that for (i, j) element of $\mathbf{A}\mathbf{A}^T$ to vanish, there exist two possibilities: the effects due to more than one mechanical transmission lines to the (i, j) element of $\mathbf{A}\mathbf{A}^T$ are equal to zero, or none of the mechanical transmission lines in the structure matrix $\mathbf{A}$ has effect to the (i, j) element of $\mathbf{A}\mathbf{A}^T$. This leads to the following axiom.

Axiom 2. For an n-dof RBR mechanism to possess the maximum acceleration capacity property at a given posture, only those structure matrices with the following characteristics can be chosen as possible gear train configurations if certain (i, j) element of the mass inertia matrix $\mathbf{M}_p$ is equal to zero: (1) more than one mechanical transmission lines have effects to the (i, j) element of $\mathbf{A}\mathbf{A}^T$, but their overall effects are equal to zero, (2) none of the mechanical transmission lines in the structure matrix $\mathbf{A}$ has effect to the (i, j) element of $\mathbf{A}\mathbf{A}^T$ and, (3) the (i, j) element of the product of $\mathbf{A}\mathbf{A}^T$ is not equal to zero if the corresponding (i, j) element of the mass inertia matrix $\mathbf{M}_p$ is not equal to zero.

Tables 3 and 4 show the admissible structure matrices for 2- and 3-dof RBR mechanisms with none of the elements in $\mathbf{M}_p$ equal to zero, and with certain element in $\mathbf{M}_p$ equal to zero at a given posture, respectively. Hence, Axioms 1 and 2 provide a rational procedure to select gear train configurations such that the maximum acceleration capacity property may be achieved with known mass inertia characteristics of the EOLC at a given posture.

Let the mass inertia matrix $\mathbf{M}_p$ of the example RBR mechanism shown in Fig. 1 take the

following form

$$\mathbf{M}_{\mathrm{p}} = \begin{bmatrix} \mathbf{M}_{\mathrm{p}}(1,1) & \mathbf{M}_{\mathrm{p}}(1,2) & \mathbf{M}_{\mathrm{p}}(1,3) \\ \mathbf{M}_{\mathrm{p}}(1,2) & \mathbf{M}_{\mathrm{p}}(2,2) & 0 \\ \mathbf{M}_{\mathrm{p}}(1,3) & 0 & \mathbf{M}_{\mathrm{p}}(3,3) \end{bmatrix} \tag{8}$$

From Table 4, there are 26 admissible structure matrices which can be selected to achieve the maximum acceleration capacity condition with $\mathbf{M}_{\mathrm{p}}(2,3)$ equal to zero. From Axioms 2, although the structure matrices with number of non-zero elements greater than number of equations are all capable to be selected as possible gear train configurations of the RBR mechanism, number of non-zero elements in the selected structure matrix is better as less as possible due to mechanical simplicity of the mechanism. Besides, motors should be located as close to the base as possible to reduce the inertia loads. Within these 26 admissible structure matrices, the g^2s^2-7 and g^2se-4 are the simplest types, while g^2s^2-7 is preferred for its better dynamic performance from the view of motor locations. The structure matrix g^2s^2-7, which has the same form as the one shown in Eq. (3), is chosen for the purpose of demonstration.

Substituting Eqs. (5a), (5b) and (8) into Eq. (6), yields

$$\mathbf{M}_{\mathrm{p}}(1,1) = I_{\mathrm{m}}\left[a_{1,1}^2 + a_{2,2}^2\right] \tag{9a}$$

$$\mathbf{M}_{\mathrm{p}}(1,2) = I_{\mathrm{m}}\left[a_{1,1}^2 \cdot b_{2,1}\right] \tag{9b}$$

$$\mathbf{M}_{\mathrm{p}}(1,3) = I_{\mathrm{m}}\left[a_{1,1}^2 \cdot b_{3,1}\right] \tag{9c}$$

$$\mathbf{M}_{\mathrm{p}}(2,2) = I_{\mathrm{m}}\left[a_{1,1}^2 \cdot b_{2,1}^2 + a_{3,3}^2 + a_{4,4}^2\right] \tag{9d}$$

$$0 = I_{\mathrm{m}}\left[a_{1,1}^2 \cdot b_{2,1} \cdot b_{3,1} + a_{3,3}^2 \cdot b_{3,3}\right] \tag{9e}$$

and

Table 3
Admissible structure matrices for 2-dof RBR mechanisms with certain zero $\mathbf{M}_{\mathrm{p}}(i,j)$

Cases	$\mathbf{M}_{\mathrm{p}}(i,j)\neq 0$	$\mathbf{M}_{\mathrm{p}}(1,2) = 0$
g^3	g^3-1	g^3-1
	g^3-2	g^3-2
g^2s	g^2s-1	g^2s-1
	g^2s-2	

Table 4
Admissible structure matrices for 3-dof RBR mechanisms with certain zero $\mathbf{M}_p(i, j)$

Cases	Non-zero $\mathbf{M}_p(i, j)$	Zero $\mathbf{M}_p(i, j)$						
		$\mathbf{M}_p(1, 2)$	$\mathbf{M}_p(1, 3)$	$\mathbf{M}_p(2, 3)$	$\mathbf{M}_p(1, 2)$; $\mathbf{M}_p(1, 3)$	$\mathbf{M}_p(1, 2)$; $\mathbf{M}_p(2, 3)$	$\mathbf{M}_p(1, 3)$; $\mathbf{M}_p(2, 3)$	$\mathbf{M}_p(1, 2)$; $\mathbf{M}_p(1, 3)$; $\mathbf{M}_p(2, 3)$
g^4	g^4-1	g^4-1	g^4-1	g^4-1	g^4-1	g^4-1	g^4-1	g^4-1
	g^4-2	g^4-2	g^4-2	g^4-2	g^4-2	g^4-2	g^4-2	g^4-2
	g^4-3	g^4-3	g^4-3	g^4-3	g^4-3	g^4-3	g^4-3	g^4-3
	g^4-4	g^4-4	g^4-4	g^4-4	g^4-4	g^4-4	g^4-4	g^4-4
	g^4-5	g^4-5	g^4-5	g^4-5	g^4-5	g^4-5	g^4-5	g^4-5
g^3s	g^3s-1	g^3s-1	g^3s-1	g^3s-1	g^3s-1	g3s-1	g^3s-1	g^3s-1
	g^3s-2	g^3s-2	g^3s-2	g^3s-2	g^3s-2	g3s-2	g^3s-2	g^3s-2
	g^3s-3	g^3s-3	g^3s-3	g^3s-3	g^3s-3	g3s-3	g^3s-3	g^3s-3
	g^3s-4	g^3s-4	g^3s-4	g^3s-4	g^3s-4	g3s-4	g^3s-4	g^3s-4
	g^3s-5	g^3s-5	g^3s-6	g^3s-5	g^3s-6	g3s-5	g^3s-6	g^3s-6
	g^3s-6	g^3s-6	g^3s-7	g^3s-6	g^3s-7	g3s-6	g^3s-7	g^3s-7
	g^3s-7	g^3s-7		g^3s-7		g^3s-7		
	g^3s-8	g^3s-8		g^3s-8		g^3s-8		
g^3e	g^3e-1	g^3e-1	g^3e-1	g^3e-1	g^3e-1	g^3e-1	g^3e-1	g^3e-1
	g^3e-2	g^3e-2	g^3e-2	g^3e-2	g^3e-2	g^3e-2	g^3e-2	g^3e-2
	g^3e-3	g^3e-3	g^3e-3	g^3e-3	g^3e-3	g^3e-3	g^3e-3	g^3e-3
	g^3e-4	g^3e-4						
	g^3e-5	g^3e-5						
g^2s^2	g^2s^2-1	g^2s^2-1	g2s2-1	g^2s^2-1	g^2s^2-1	g^2s^2-1	g^2s^2-1	g^2s^2-1
	g^2s^2-2	g^2s^2-2	g2s2-2	g^2s^2-2	g^2s^2-2	g^2s^2-2	g^2s^2-2	g^2s^2-2
	g^2s^2-3	g^2s^2-3	g2s2-5	g^2s^2-3	g^2s^2-5	g^2s^2-3	g^2s^2-5	g^2s^2-5
	g^2s^2-4	g^2s^2-4	g2s2-8	g^2s^2-4		g^2s^2-4	g^2s^2-8	
	g^2s^2-5			g^2s^2-5				
	g^2s^2-6			g^2s^2-6				
	g^2s^2-7			g^2s^2-7				
g^2se	g^2se-1	g^2se-1	g^2se-1	g^2se-1	g^2se-1	g^2se-1	g^2se-1	g^2se-1
	g^2se-2	g^2se-2	g^2se-2	g^2se-2	g^2se-2	g^2se-2	g^2se-2	g^2se-2
	g^2se-3	g^2se-3	g^2se-6	g^2se-3	g^2se-6	g^2se-3		
	g^2se-4	g^2se-5	g^2se-7	g^2se-4				
	g^2se-5							

$$\mathbf{M}_{\mathrm{p}}(3,3) = I_{\mathrm{m}}\left[a_{11}^2 \cdot b_{3,1}^2 + a_{3,3}^2 \cdot b_{3,3}^2\right] \tag{9f}$$

5. Sign relations

5.1. The inner structure matrix

From Eq. (9e), the signs among $b_{2,1}$, $b_{3,1}$, and $b_{3,3}$ can be related as

$$\mathrm{sign}\left(\frac{b_{2,1} \cdot b_{3,1}}{b_{3,3}}\right) = - \tag{10}$$

Table 5 shows the four possible sign combinations of $b_{2,1}$, $b_{3,1}$, and $b_{3,3}$ according to Eq. (10). It can be seen that from Eq. (9b), the sign of $b_{2,1}$ is synchronized with that of $\mathbf{M}_{\mathrm{p}}(1,2)$, while the sign of $b_{3,1}$ is synchronized with that of $\mathbf{M}_{\mathrm{p}}(1,3)$ from Eq. (9c). Hence, with the inertia matrix $\mathbf{M}_{\mathrm{p}}$ at a given posture, signs of elements of the inner structure matrix can be determined. For the purpose of demonstration, let $\mathbf{M}_{\mathrm{p}}(1,2)$ and $\mathbf{M}_{\mathrm{p}}(1,3)$ be both negative for the example RBR mechanism, and signs of elements of the inner structure matrix are selected as case (d) in Table 5 and can be expressed as

$$\mathrm{sign}(b_{2,1}) = \mathrm{sign}(\gamma_{7,6'}) = - \tag{11}$$

$$\mathrm{sign}(b_{3,1}) = \mathrm{sign}(\gamma_{7,6'} \cdot \gamma_{11,7'} \cdot \gamma_{3,11'}) = - \tag{12}$$

$$\mathrm{sign}(b_{3,3}) = \mathrm{sign}(\gamma_{3',10'}) = - \tag{13}$$

From Eqs. (11) and (12), we have

$$\mathrm{sign}(\gamma_{11,7'} \cdot \gamma_{3,11'}) = + \tag{14}$$

From Eq. (11), since sign of $\gamma_{7,6'}$ is negative, link 7 is to be designed to rotate negatively while link 6 rotates positively. Since sign of $\gamma_{3',10'}$ is negative, from Eq. (13), link 3 is to be designed to rotate negatively while link 10 rotates positively. From Eq. (14), since sign of $\gamma_{11,7'} \cdot \gamma_{3,11'}$ is positive, link 3 is to be designed to rotate positively while link 7 rotates positively. Hence, with

Table 5
Admissible sign relations between elements of the inner structure matrix

	$b_{2,1}$	$b_{3,1}$	$b_{3,3}$
(a)	+	+	−
(b)	+	−	+
(c)	−	+	+
(d)	−	−	−

these determined sign relations, admissible gearing configurations associated with inner structure of the RBR mechanism can be determined. Fig. 3 shows one of the possible drive train arrangements.

5.2. The outer structure matrix

For RBR mechanisms, since backlash can be eliminated by applying opposite unidirectional torques on each joint of the EOLC, partial torques associated with any joint torque must not be all of the same direction. From Eqs. (2), (5a) and (5b), resultant torques at joint-space can be written as the sum of their associated partial torques. By substituting Eqs. (5a) and (5b) into Eq. (2) and by considering the selected signs of $b_{j,k}$'s in Eqs. (11)–(13), resultant joint torques can be written as

$$\tau_{10} = a_{1,1}\xi_4 + a_{2,2}\xi_5 \tag{15}$$

$$\tau_{21} = -a_{1,1}\xi_4 + a_{3,3}\xi_8 + a_{4,4}\xi_9 \tag{16}$$

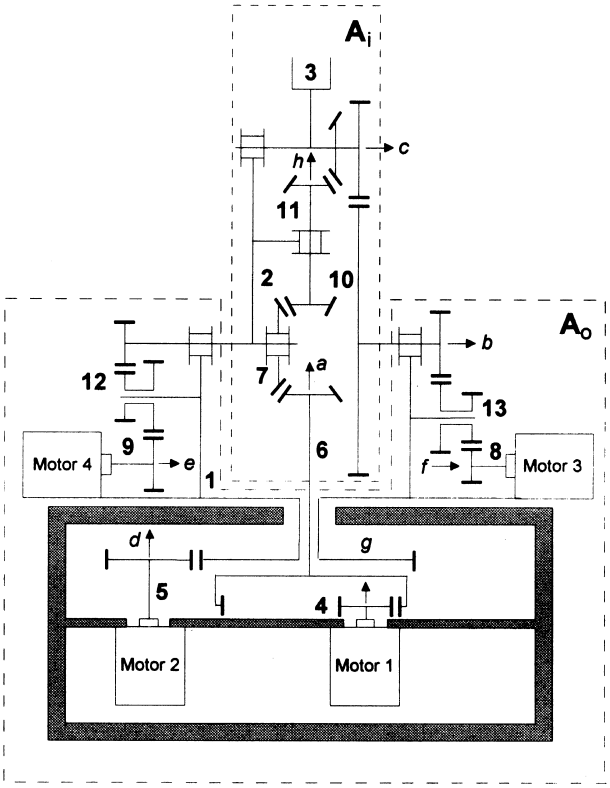

Fig. 3. A possible gearing configuration.

$$\tau_{32} = -a_{1,\,1}\xi_4 - a_{3,\,3}\xi_8 \tag{17}$$

From Eqs. (15) and (17), it can be seen that joint torque τ_{10} is composed of partial torques $a_{1,\,1}\xi_4$ and $a_{2,\,2}\xi_5$, while τ_{32} is composed of partial torques $-a_{1,\,1}\xi_4$ and $-a_{3,\,3}\xi_8$. Hence, signs of $a_{1,\,1}\xi_4$ and $a_{2,\,2}\xi_5$ and that of $a_{1,1}\xi_4$ and $a_{3,\,3}\xi_8$ must be different, i.e.

$$\operatorname{sign}(a_{1,\,1}\xi_4) = -\operatorname{sign}(a_{2,\,2}\xi_5) \tag{18}$$

$$\operatorname{sign}(a_{1,\,1}\xi_4) = -\operatorname{sign}(a_{3,\,3}\xi_8) \tag{19}$$

From Eq. (16), it can also be seen that all partial torques of τ_{21}, $-a_{1,\,1}\xi_4$, $a_{3,\,3}\xi_8$, and $a_{4,\,4}\xi_9$, cannot be of the same sign. Thus, from Eqs. (16) and (19), we have

$$\operatorname{sign}(a_{1,\,1}\xi_4) = \operatorname{sign}(a_{4,\,4}\xi_9) \tag{20}$$

Assuming that motors 1, 2, 3, and 4 rotate in counterclockwise direction, from Fig. 1, it can be seen that the motors 1, 2, and 4 rotate positively along their axes of rotation while motor 3 rotates negatively along its axis of rotation. The directions of motor torques, ξ_4, ξ_5, ξ_8, and ξ_9 can be expressed as

$$\operatorname{sign}(\xi_4, \xi_5, \xi_8, \xi_9) = (+, +, -, +) \tag{21}$$

Thus, from Eqs. (18)–(21), sign relations among elements of the outer structure matrix can be derived as

$$\operatorname{sign}(a_{1,\,1}) = -\operatorname{sign}(a_{2,\,2}) \tag{22}$$

$$\operatorname{sign}(a_{1,\,1}) = +\operatorname{sign}(a_{3,\,3}) \tag{23}$$

and

$$\operatorname{sign}(a_{1,\,1}) = -\operatorname{sign}(a_{4,\,4}) \tag{24}$$

Table 6 shows two admissible sign combinations of elements of the outer structure matrix. For the purpose of demonstration, case (a) is selected. Thus, we have

$$\operatorname{sign}(a_{1,\,1}) = \operatorname{sign}(\gamma_{6,\,4}) = + \tag{25a}$$

$$\operatorname{sign}(a_{2,\,2}) = \operatorname{sign}(\gamma_{1,\,5}) = - \tag{25b}$$

Table 6
Admissible sign relations between elements of the outer structure matrix

	$a_{1,\,1}$	$a_{2,\,2}$	$a_{3,\,3}$	$a_{4,\,4}$
(a)	+	−	+	+
(b)	−	+	−	−

$$\text{sign}(a_{3,3}) = \text{sign}(\gamma_{10,8}) = + \tag{25c}$$

$$\text{sign}(a_{4,4}) = \text{sign}(\gamma_{2,9}) = + \tag{25d}$$

From Eq. (25a), since sign of $\gamma_{6,4}$ is positive, link 6 is to be designed to rotate positively while link 4 rotates positively. Since sign of $\gamma_{1,5}$ is negative, from Eq. (25b), link 1 is to be designed to rotate negatively while link 5 rotates positively. From Eqs. (25c) and (25d), since signs of both $\gamma_{10,8}$ and $\gamma_{2,9}$ are positive, links 10 and 2 are to be designed to rotate positively while links 8 and 9 rotate positively, respectively.

Note that for the case where to use several gear stages is desirable rather than a single stage to adjust the center distance and/or to adjust the sign relation between rotational axes, idle gear(s) can be added. Hence, with these selected signs of elements of the outer structure matrix, the use of internal/external gear pairs can be decided accordingly. Fig. 3 shows one of the possible drive train arrangements. Note that in Fig. 3, links 12 and 13 are added as idlers to relocate the input motors. Thus, we have

$$a_{3,3} = \gamma_{10,8} = \gamma_{10,13'} \cdot \gamma_{13,8} \tag{26}$$

and

$$a_{4,4} = \gamma_{2,9} = \gamma_{2,12'} \cdot \gamma_{12,9} \tag{27}$$

6. Determination of gear ratios

By solving Eqs. (9a)–(9f), elements of the inner and outer structure matrices can be determined as

$$b_{2,1} = \frac{1}{(k^2+1)} \frac{\mathbf{M}_{\mathrm{p}}(1,2) \cdot \mathbf{M}_{\mathrm{p}}(3,3)}{\mathbf{M}_{\mathrm{p}}^2(1,3)} \tag{28a}$$

$$b_{3,1} = \frac{1}{(k^2+1)} \frac{\mathbf{M}_{\mathrm{p}}(3,3)}{\mathbf{M}_{\mathrm{p}}(1,3)} \tag{28b}$$

$$b_{3,3} = -k^2 \frac{\mathbf{M}_{\mathrm{p}}(1,3)}{\mathbf{M}_{\mathrm{p}}(1,2)} \tag{28c}$$

$$a_{1,1}^2 = \left(k^2+1\right) \frac{\mathbf{M}_{\mathrm{p}}^2(1,3)}{I_{\mathrm{m}} \cdot \mathbf{M}_{\mathrm{p}}(3,3)} \tag{28d}$$

$$a_{2,2}^2 = \frac{\mathbf{M}_{\mathrm{p}}(1,1)}{I_{\mathrm{m}}} - \left(k^2+1\right) \frac{\mathbf{M}_{\mathrm{p}}^2(1,3)}{I_{\mathrm{m}} \cdot \mathbf{M}_{\mathrm{p}}(3,3)} \tag{28e}$$

$$a_{3,3}^2 = \frac{1}{k^2(k^2+1)} \frac{\mathbf{M}_p(1,2) \cdot \mathbf{M}_p(3,3)}{I_m \cdot \mathbf{M}_p^2(1,3)} \tag{28f}$$

and

$$a_{4,4}^2 = \frac{\mathbf{M}_p(2,2)}{I_m} - \frac{1}{k^2} \frac{\mathbf{M}_p^2(1,2) \cdot \mathbf{M}_p(3,3)}{\mathbf{M}_p^2(1,3)} \tag{28g}$$

where

$$k = a_{3,3} b_{3,3} / a_{1,1} b_{3,1} \tag{29}$$

Note that since left-hand sides of Eqs. (28e) and (28g) are of quadratic form, their associated right-hand sides are positive. From Eq. (28e), we have

$$k^2 < \frac{\mathbf{M}_p(1,1) \cdot \mathbf{M}_p(3,3)}{\mathbf{M}_p(1,3)} - 1 \tag{30}$$

From Eq. (28g), we have

$$k^2 > \frac{\mathbf{M}_p^2(1,2) \cdot \mathbf{M}_p(3,3)}{\mathbf{M}_p^2(1,3) \cdot \mathbf{M}_p(2,2)} \tag{31}$$

From Eqs. (30) and (31), the range of k can be defined with given inertia properties of primary links. Thus, elements of the inner and outer structure matrices can be determined with a proper choice of k. For the purpose of demonstration, let inertia matrix of primary links be given by

$$\mathbf{M}_p = \begin{bmatrix} 20{,}000 & -7000 & -9000 \\ -7000 & 30{,}000 & 0 \\ -9000 & 0 & 40{,}000 \end{bmatrix} \left(10^{-7}\ \mathrm{kg\ m^2}\right) \tag{32}$$

By substituting corresponding elements of Eq. (32) into Eqs. (30) and (31), the range of k can be determined as

$$0.81 < k^2 < 8.88 \tag{33}$$

For the case $k^2 = 1$, by substituting Eq. (32) into Eqs. (28a)–(28c), elements of the inner structure matrix can be determined as

$$b_{2,1} = \gamma_{7,6'} = -1.73 \tag{34a}$$

$$b_{3,1} = \gamma_{7,6'} \cdot \gamma_{11,7'} \cdot \gamma_{3,11'} = -2.22 \tag{34b}$$

$$b_{3,3} = \gamma_{3',10'} = -1.29 \tag{34c}$$

Thus,

$$\mathbf{A}_{\mathrm{i}} = \begin{bmatrix} 1 & 1 & 0 & 0 \\ -1.73 & 0 & 1 & 1 \\ -2.22 & 0 & -1.29 & 0 \end{bmatrix} \tag{35}$$

Let $I_i = 1 \times 10^{-5}$ kg/m^2 ($i = 1, 2, 3, 4$) for the input links. By substituting Eq. (32) into Eqs. (28d)–(28g), and with the selected sign relations, elements of the outer structure matrix can be determined as

$$a_{1,1} = \gamma_{6,4} = 6.36 \tag{36a}$$

$$a_{2,2} = \gamma_{1,5} = -12.63 \tag{36b}$$

$$a_{3,3} = \gamma_{10,13'} \cdot \gamma_{13,8} = 11.00 \tag{36c}$$

$$a_{4,4} = \gamma_{2,12'} \cdot \gamma_{12,9} = 7.62 \tag{36d}$$

Thus,

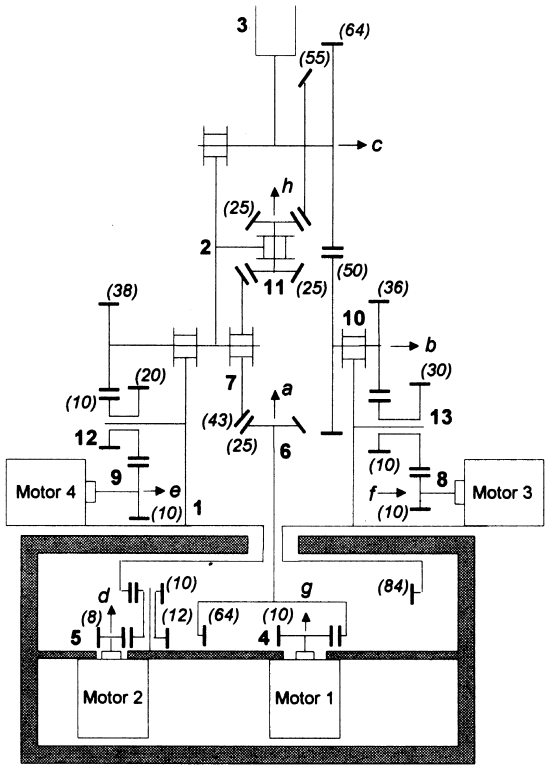

Fig. 4. A possible RBR mechanism.

$$\mathbf{A}_o = \begin{bmatrix} 6.36 & 0 & 0 & 0 \\ 0 & -12.63 & 0 & 0 \\ 0 & 0 & 11.00 & 0 \\ 0 & 0 & 0 & 7.62 \end{bmatrix} \tag{37}$$

From Eqs. (35), (37) and (4), structure matrix **A** of the example RBR mechanism can be shown as

$$\mathbf{A} = \begin{bmatrix} 6.36 & -12.63 & 0 & 0 \\ -11.00 & 0 & 11.00 & 7.62 \\ -14.12 & 0 & -14.19 & 0 \end{bmatrix} \tag{38}$$

Several methods [1,9,10] have been developed to find the teeth number of each gear pair to provide a specific ratio. Fig. 4 shows a possible gear train arrangement of the example RBR mechanism by selecting the gear ratios as close to the optimal values as possible. Note that in Fig. 4, link 14 is added as an idler such that two-stage gear reductions are desirable rather than a single stage.

7. Conclusion

This paper describes a systematic methodology for the drive train design of RBR mechanisms. The approach is based on the idea that the structure matrix of an n-dof RBR mechanism can be decomposed as the product of inner and outer structure matrices. The drive train design problem is treated as a two-stage procedure. In the first stage, gearing configurations of the drive train are determined from the sign relations among elements of inner and outer structure matrices. In the second stage, the associated gear ratios are determined from the maximum acceleration capacity condition. The design procedure can be summarized as follows:

1. With the given inertia properties of primary links and the form of its associated inertia matrix, $\mathbf{M}_p$, select proper form of structure matrix from Table 3 or Table 4.
2. Derive admissible sign relations among elements of the inner structure matrix from the signs of $\mathbf{M}_p$ and the generalized principle of inertia match.
3. Derive admissible sign relations among elements of the outer structure matrix based on the unidirectional drive characteristics of RBR mechanisms.
4. Derive the gearing configurations of drive trains according to the selected sign relations among elements on the inner and outer structure matrices.
5. Determine gear ratios of the elements in the inner and outer structure matrices from the maximum acceleration capacity condition.
6. Complete the drive train design by adding idlers to adjust the center distance between axes or to relocate the motors.

References

[1] A. Arabyan, G.R. Shiflett, ASME Journal of Mechanisms, Transmissions, and Automation in Design 109 (1987) 475.
[2] S.L. Chang, L.W. Tsai, IEEE International Journal of Robotics and Automation 6 (1) (1990) 97.
[3] S.L. Chang, L.W. Tsai, ASME Journal of Mechanical Design 115 (1993) 247.
[4] D.Z. Chen, Journal of Chinese Society of Mechanical Engineers 16 (1) (1995) 29.
[5] D.Z. Chen, Journal of Robotic Systems 14 (8) (1997) 601.
[6] D.Z. Chen, L.W. Tsai, ASME Journal of Mechanical Design 115 (1993) 241.
[7] D.Z. Chen, L.W. Tsai, Journal of Applied Mechanisms and Robotics 1 (3) (1994) 17.
[8] D.Z. Chen, S.C. Wang, Mechanism and Machine Theory 34 (1) (1999) 105.
[9] Dil Pare AL. ASME Journal of Engineering for Industry 1971:196.
[10] W.C. Orthwein, ASME Journal of Mechanical Design 104 (1982) 775.
[11] L.W. Tsai, IEEE Journal of Robotics and Automation 4 (2) (1988) 150.